Heterogeneous Hydrogenation

DOI: 10.1002/anie.200702274

Bimetallic Ru–Sn Nanoparticle Catalysts for the Solvent-Free Selective Hydrogenation of 1,5,9-Cyclododecatriene to Cyclododecene**

Richard D. Adams, Erin M. Boswell, Burjor Captain, Ana B. Hungria, Paul A. Midgley, Robert Raja,* and John Meurig Thomas**

Cyclododecene (CD) is an important intermediate in the chemical industry since it figures eminently in the synthesis of dicarboxylic aliphatic acids, ketones, cyclic alcohols, lactones and other useful materials, including 12-laurolactam and dodecanedioic acid which are monomers used in the manufacture of nylon 12, nylon 612, copolyamides and polyesters all of which have extensive applications.

Two of us previously reported[1] that cyclododecene may be efficiently produced in a low-temperature, solvent-free fashion by selectively hydrogenating 1,5,9-cyclododecatriene (CDT) in the presence of a Ru_6Sn nanoparticle catalyst. The actual catalyst was derived[2] from the precursor carbonylate $[Ru_6C(CO)_{16}SnCl_3]^-$, in which the chlorinated tin atom bridges two of the six ruthenium atoms of the octahedral cluster.[3] From in situ extended X-ray absorption fine structure (EXAFS) and FTIR studies[1] on the denuded active Ru_6Sn nanoparticle catalyst it was clear a residual chlorine atom remained attached to the active catalytic entity (see Figure 3 of Ref. [1]).

Conscious of the known modifying effect of Sn on Ru (and other) catalysts,[1,4] and also of the difficulties, such as reproducibility, frequently associated with the presence of chlorine in supported catalysts,[5] we have set about to prepare a range of new Ru–Sn carbonyl complexes for use as catalyst precursors that are free of Cl (and also of the carbidic carbon), present in the previously reported active catalyst.[3] In evolving a suitable method of preparation, we have arrived at a means of systematically altering the Ru:Sn ratios in bimetallic nanoparticles, consisting of clusters with a total atom content of as little as two and as large as ten atoms.

Herein we describe the synthesis and structures of four new tin-containing tetraruthenium cluster complexes, two of which we have tested in their denuded form and have found to be active catalysts for the highly selective hydrogenation of CDT to CD. The compounds $[Ru_4(\mu_4\text{-}SnPh)_2(CO)_{12}]$ (**1**), $[Ru_4(\mu_4\text{-}SnPh)_2(\mu\text{-}SnPh_2)_2(\mu\text{-}CO)_2(CO)_8]$ (**2**), $[Ru_4(\mu_4\text{-}SnPh)_2(\mu\text{-}SnPh_2)_3(\mu\text{-}CO)(CO)_8]$ (**3**), and $[Ru_4(\mu_4\text{-}SnPh)_2(\mu\text{-}SnPh_2)_4(CO)_8]$ (**4**) were obtained from the reaction of $[Ru_4(CO)_{12}(\mu\text{-}H)_4]$ with Ph_3SnH in octane solvent at reflux (125 °C; Scheme 1). All four compounds were characterized by a combination of IR and ^1H NMR spectroscopy, single-crystal X-ray diffraction, and mass spectrometry.

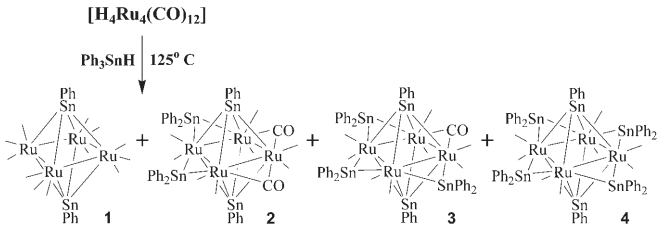

Scheme 1.

Each compound contains an approximately square-planar cluster of four ruthenium atoms with two quadruply bridging SnPh ligands, one on each side of the Ru_4 square (Scheme 1). The molecular structures of **1** and **4** are shown in Figures 1 and 2, respectively. Compound **1** contains twelve carbonyl ligands like its parent compound, whereas in compounds **2**–**4**, two, three, and four of the CO ligands were replaced by $SnPh_2$ groups that bridge the Ru–Ru edges of the Ru_4 square. The μ_4-SnPh stannylyne ligands present in these clusters are very rare. In fact, there is only one reported example of a μ_4-SnPh ligand; this was observed for the compound $[Ru_5(CO)_{11}(\eta^6\text{-}C_6H_6)(\mu_4\text{-}SnPh)(\mu_3\text{-}CPh)]$.[6]

Compounds **1**, **2**, and **4** were chosen for our catalytic investigations. The compounds were deposited (ca. 2 % metal loading) on Davison 923 silica mesopore (38 Å) and were activated by heating to 200 °C for 2 h in vacuum. Catalytic tests were carried out as described in the Experimental Section. A typical kinetic plot for the hydrogenation of CDT at 393 K by the Ru_4Sn_6 catalyst supported on mesoporous silica is shown in Figure 3.

A comparison of the performance of the three new bimetallic RuSn nanoparticle catalysts with one another, with the Ru_6Sn (chlorine-containing) catalyst, and with Ru_5PtSn[7]

[*] Prof. Dr. R. D. Adams, E. M. Boswell, Dr. B. Captain
Department of Chemistry and Biochemistry
University of South Carolina
Columbia, SC 29208 (USA)
Fax: (+1) 803-777-6781
E-mail: adams@mail.chem.sc.edu
Prof. Dr. R. Raja
School of Chemistry, University of Southampton
Highfield, Southampton SO171BJ (UK)
E-mail: r.raja@soton.ac.uk
Dr. A. B. Hungria, Dr. P. A. Midgley, Prof. Sir J. M. Thomas
Department of Materials Science, University of Cambridge
Cambridge CB23QZ (UK)
Fax: (+44) 1223-334-563
E-mail: jmt2@cam.ac.uk

[**] This research was supported by the Office of Basic Energy Sciences of the U.S. Department of Energy under Grant No. DE-FG02-00ER14980.

Supporting information for this article is available on the WWW under http://www.angewandte.org or from the author.

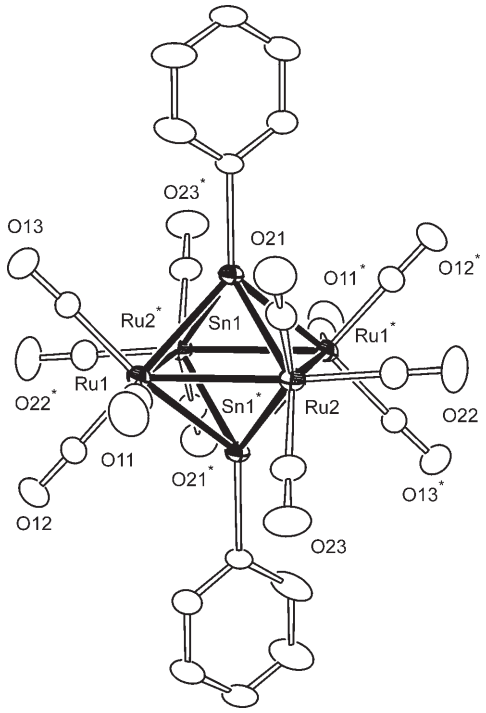

Figure 1. An ORTEP diagram of **1** (thermal ellipsoids set at 30% probability). Selected bond lengths [Å]: Ru1–Ru2 2.9578(6), Ru1–Ru2* 2.9597(6), Ru1–Sn1 2.7135(5), Ru1–Sn1 2.7147(5), Ru2–Sn1 2.7153(6), Ru2–Sn1* 2.7134(5).

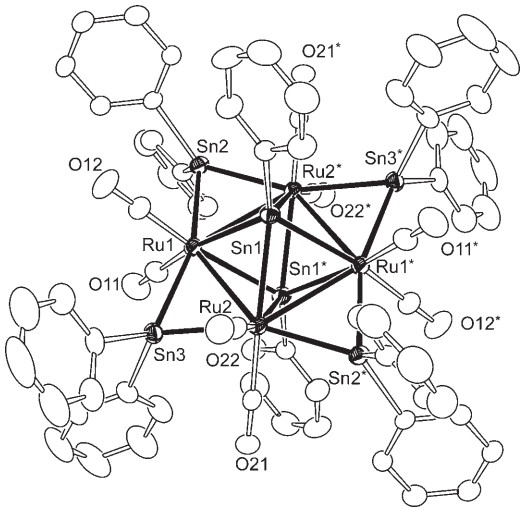

Figure 2. An ORTEP diagram of **4** (thermal ellipsoids set at 30% probability). Selected bond lengths [Å]: Ru1–Ru2 2.9578(6), Ru1–Ru2* 2.9597(6), Ru1–Sn1 2.7135(5), Ru1–Sn1 2.7147(5), Ru2–Sn1 2.7153(6), Ru2–Sn1* 2.7134(5).

is shown in Figure 4. Both in regard to degree of conversion and with respect to selectivity towards formation of the desirable CD, the Ru_4Sn_6 preparation surpasses the performance of both Ru_4Sn_2 and Ru_6Sn. It is also noteworthy that, as seen in Figure 5, a substantial increase in conversion (with close to 100% selectivity) occurs when the reaction is carried out at 413 K.

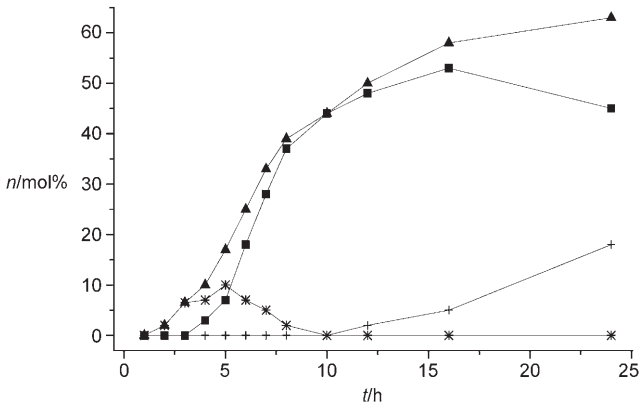

Figure 3. Kinetic plot for the hydrogenation of 1,5,9-cyclododecatriene using Ru_4Sn_6 at 393 K (▲ conversion; * 1,9-cyclododecadiene; ■ cyclododecene; + cyclododecane). At 393 K, and under 30 bar H_2 the solvent-free conversion of 1,5,9-cyclododecatriene into cyclododecene proceeds smoothly, and for the first 12 h almost exclusively, in the presence of the Ru_4Sn_6 bimetallic nanoparticle catalyst supported on mesoporous silica. *n*/mol% represents the conversion (%) into product.

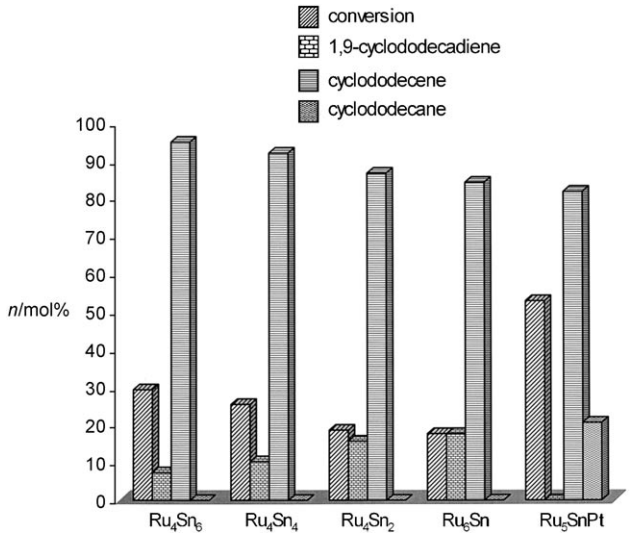

Figure 4. Comparison of catalytic performance of Ru_4Sn_6, Ru_4Sn_4, Ru_4Sn_2, and Ru_5SnPt with the previously reported (chlorine-containing) Ru_6Sn. Reaction conditions: substrate 50 g, catalyst 25 mg (cluster anchored on mesopore 2% metal loading), H_2 pressure 30 bar, $T = 373$ K, $t = 8$ h. *n*/mol% represents the conversion (%) into product.

The catalysts were characterized both before and after catalysis by scanning transmission electron microscopy (STEM). An image showing the nanoparticles derived from **4** after catalysis is shown in Figure 6. It can be seen that the metal particles are very small and are uniformly approximately 1 nm in size, allowing for the enlargement in appearance that results from electron optical effects.[8] Energy dispersive X-ray (EDX) analysis by scanning electron microscopy (SEM) shows that the composition of each of the supported catalysts is very similar to the composition of its molecular precursor.

Our results demonstrate not only the superiority of using bimetallic carbonyl complexes as precursors to provide highly

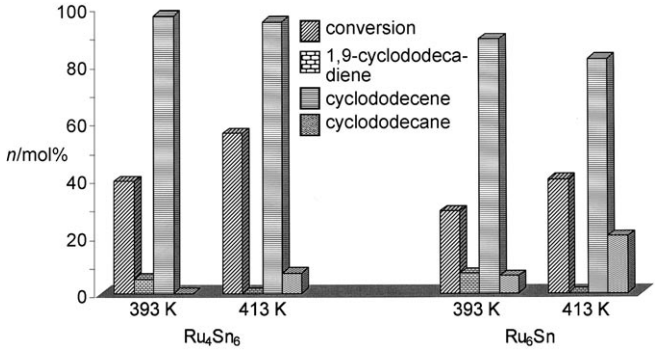

Figure 5. The superiority of the Ru_4Sn_6 bimetallic catalyst over the previously reported Ru_6Sn in the production of the cyclododecene from the cyclodecatriene is illustrated (as a function of temperature). Reaction conditions: substrate approximately 50 g, catalyst approximately 25 mg (cluster anchored on mesopore approximately 2% metal loading), H_2 pressure approximately 30 bar, $t = 8$ h. *n*/mol% represents the conversion (%) into product.

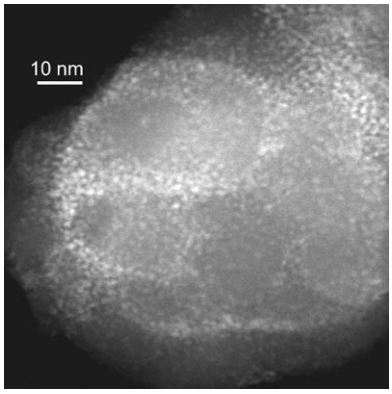

Figure 6. High-angle annular dark-field (HAADF) images of Ru_4Sn_6 nanoclusters on Davison 38 Å silica after CDT hydrogenation catalysis.

dispersed supported naked bimetallic catalysts, but also the beneficial effects of the tin modifier on enhancing the selectivity. There is clearly much scope to enhance further the catalytic performance of Ru–Sn bimetallic catalysts (by exploring other ratios of Ru:Sn and other structures of precursor entities (from 1:1 to 1:5 of Sn:Ru)). Moreover, it is likely that addition of Pt to form trimetallic nanoparticle catalysts, as was done in the case of Ru_5PtSn,[7] will yield particularly powerful new, solvent-free hydrogenation catalysts for which there will be much demand in the emerging hydrogen economy.[9]

Experimental Section

$[Ru_4(CO)_{12}(\mu\text{-}H)_4]$ with Ph_3SnH at 125 °C: Ph_3SnH (53 mg, 0.151 mmol) was added to a solution of $[Ru_4(CO)_{12}(\mu\text{-}H)_4]$ (25 mg, 0.033 mmol) in distilled octane (20 mL). The reaction mixture was heated to reflux for 20 min, after which the solvent was removed in vacuum. The residue was extracted with methylene chloride and separated by thin-layer chromatography (TLC) over silica gel using a 3:1 (v/v) hexane/methylene chloride solvent mixture to yield in order of elution 1.7 mg (4%) of lilac $[Ru_4(\mu_4\text{-}SnPh)_2(CO)_{12}]$ (**1**), 1.3 mg (2%) of purple $[Ru_4(\mu_4\text{-}SnPh)_2(\mu\text{-}SnPh_2)_2(\mu\text{-}CO)_2(CO)_8]$ (**2**), 2.8 mg (4%) of purple $[Ru_4(\mu_4\text{-}SnPh)_2(\mu\text{-}SnPh_2)_3(\mu\text{-}CO)(CO)_8]$ (**3**), and 5.4 mg (7%) of blue $[Ru_4(\mu_4\text{-}SnPh)_2(\mu\text{-}SnPh_2)_4(CO)_8]$ (**4**). Spectral data for **1**: IR(ν_{CO}): $\tilde{\nu} = 2045$(vs), 2001(s) cm^{-1}. ^1H NMR (C_6D_6): $\delta =$ 7.00–7.08 (m, 6H), 7.58–7.62 ppm (m, 4H). EI/MS: *m*/*z* 1131. The isotope pattern is consistent with the presence of four ruthenium and two tin atoms. Spectral data for **2**: IR(ν_{CO}): $\tilde{\nu} = 2057$(s), 2021(vs), 1998(s), 1983(s,sh), 1959(w), 1844(w), 1821(w) cm^{-1}. ^1H NMR (C_6D_6): $\delta = 6.90$–7.20 (m, 10H), 7.21–7.40 (m, 16H), 7.66–7.71 ppm (m, 4H). EI/MS: *m*/*z* 1621. The isotope pattern is consistent with the presence of four ruthenium and four tin atoms. Spectral data for **3**: IR(ν_{CO}): $\tilde{\nu} =$ 2058(w), 2039(m), 2017(m), 2002(vs), 1989(s), 1958(m), 1822(w) cm^{-1}. ^1H NMR (C_6D_6): $\delta = 7.04$–7.08 (m, 3H), 7.28–7.42 (m, 28H), 7.65–7.72 ppm (m, 9H). EI/MS: *m*/*z* 1866. The isotope pattern is consistent with the presence of four ruthenium and five tin atoms. Spectral data for **4**: IR(ν_{CO}): $\tilde{\nu} = 1996$(vs), 1962(s) cm^{-1}. ^1H NMR (C_6D_6): $\delta = 6.87$–6.89 (m, 4H), 7.20–7.32 (m, 30H), 7.63–7.66 ppm (m, 16H). EI/MS: *m*/*z* 2111. The isotope pattern is consistent with the presence of four ruthenium and six tin atoms. Crystal data for **1**: $Ru_4Sn_2O_{12}C_{24}H_{10}$, $M_r = 1131.98$, triclinic, space group $P\bar{1}$, $a = 9.1416(4)$, $b = 9.6670(4)$, $c = 9.7105(4)$ Å, $\alpha = 74.889(1)$, $\beta = 66.258(1)$, $\gamma = 86.839(1)°$, $V = 757.16(6)$ Å^3, $Z = 1$, $T = 294$ K, $Mo_{K\alpha} = 0.71073$ Å, $2\Theta_{max} = 56.62°$, GOF = 1.073. The final $R1(F^2)$ was 0.0358 for 3202 reflections $I > 2\sigma(I)$. Crystal data for **2**: $Ru_4Sn_4O_{10}C_{46}H_{30}$, $M_r = 1621.74$, triclinic, space group $P\bar{1}$, $a =$ 11.8757(6), $b = 12.9166(7)$, $c = 18.0535(9)$ Å, $\alpha = 80.993(1)$, $\beta =$ 81.988(1), $\gamma = 66.009(1)°$, $V = 2490.0(2)$ Å^3, $Z = 2$, $T = 294$ K, $Mo_{K\alpha} = 0.71073$ Å, $2\Theta_{max} = 56.70°$, GOF = 1.024. The final $R1(F^2)$ was 0.0354 for 10078 reflections $I > 2\sigma(I)$. Crystal data for **3**: $Ru_4Sn_5O_9C_{57}H_{40}$, $Mr = 1866.62$, triclinic, space group $P\bar{1}$, $a =$ 13.3973(3), $b = 13.8172(3)$, $c = 17.8555(4)$ Å, $\alpha = 89.312(1)$, $\beta =$ 89.351(1), $\gamma = 64.805(1)°$, $V = 2990.55(11)$ Å^3, $Z = 2$, $T = 294$ K, $Mo_{K\alpha} = 0.71073$ Å, $2\Theta_{max} = 56.60°$, GOF = 1.021. The final $R1(F^2)$ was 0.0405 for 10690 reflections $I > 2\sigma(I)$. Crystal data for **4**: $Ru_4Sn_6O_8C_{68}H_{50}$, $M_r = 2111.50$, triclinic, space group $P\bar{1}$, $a =$ 11.9551(5), $b = 12.3520(5)$, $c = 12.6818(5)$ Å, $\alpha = 78.933(1)$, $\beta =$ 70.662(1), $\gamma = 75.589(1)°$, $V = 1699.12(12)$ Å^3, $Z = 1$, $T = 294$ K, $Mo_{K\alpha} = 0.71073$ Å, $2\Theta_{max} = 56.58°$, GOF = 0.988. The final $R1(F^2)$ was 0.0322 for 6452 reflections $I > 2\sigma(I)$. CCDC-659926–CCDC-659929 contain the supplementary crystallographic data for this paper. These data can be obtained free of charge from The Cambridge Crystallographic Data Centre via www.ccdc.cam.ac.uk/data_request/cif

Conversion of **3** into **4**. Ph_3SnH (5.7 mg, 0.003 mmol) was added to a suspension of **3** in nonane (25 mL). The reaction mixture was heated to reflux for 2 h, after which the solvent was removed in vacuum. The residue was extracted with methylene chloride and separated by TLC over silica gel using a 3:1 (v/v) hexane/methylene chloride solvent mixture to yield 1.1 mg (16%) of **4**.

Preparation of the catalysts: **1** (13.0 mg) was dissolved in of CH_2Cl_2 (10 mL). Davison mesoporous silica (400 mg; Grace Davison, designated Davison 923, having a pore diameter of 38 Å) was added to this solution and the solvent was removed under a slow stream of N_2. The support (with anchored cluster) was activated (decarbonylated) by calcination in vacuum by heating to 200 °C over a period of approximately 45 min and then maintained at 200 °C for an additional 2 h. Similarly compound **4** was anchored on Davison mesoporous silica.

Catalysis: The catalytic testing was carried out with a high-pressure stainless reactor (Cambridge Reactor Design) lined with polyether ether ketone (PEEK). Nanoparticle Ru–Sn catalysts supported on Davison mesoporous silica (mean diameter 38 Å) (25 mg) were activated (473 K, 2 h) in the presence of hydrogen (0.5 MPa) prior to the hydrogenation of the 1,5,9-cyclododecatriene. The catalysts were introduced into the reactor using a roboter controlled, custom-built catalyst delivery unit, in order to minimize exposure to air. The reactor was then depressurized and cooled to room temperature, before introducing the reactant (50 g) and internal standard (octane, 2.5 g). After introducing the reactant and internal

standard, the reactor was purged three times with dry nitrogen prior to the introduction of H_2. The reaction vessel was pressurized with hydrogen (30 bar, dynamic) and heated to the desired temperature with continued stirring (1200 rpm). During the reaction, small aliquots were removed by using a mini-robot autosampler to enable the kinetics to be studied (see Figure 3). The products of the reaction were analyzed with gas chromatography (G.C. Varian Model 3400 CX) employing a HP-1 capillary column (25 m × 0.32 mm) and flame ionization detector. The identity of the products was confirmed by LC-MS (Shimadzu, QP 8000).

Both the Ru_4Sn_6 and Ru_4Sn_2 bimetallic, supported catalysts, were reused six or seven times for the hydrogenation of the parent CDT without any significant loss in catalytic activity or selectivity, and our standard procedure[1a] was employed to test for (and establish) any leaching, which was infinitesimal.

The conversions and selectivities were determined as defined by the following equations and the yields were normalized with respect to the response factors obtained as above: Conv. (%) = [(mol of initial substrate − mol of residual substrate)/(mol of initial substrate)] × 100. Sel. (%) = [(mol of individual product)/(mol of total products)] × 100.

For the internal standard GC method, the response factor (RF), and mol % of individual products were calculated using the following equations: RF = (mol product/mol standard) × (area standard/area product). Mol % product = RF × mol standard × (area product/area standard) × 100/mol sample.

Electron microscopy. High-angle annular dark-field (HAADF) images were recorded on a 200 kV FEI Tecnai STEM/TEM electron microscope. Specimens were prepared by crushing the catalyst between glass slides and depositing the resulting powder onto a copper grid supporting a perforated carbon film. Deposition was achieved by dipping the grid directly into the sample powder to avoid possible contact with any solvent. X-ray energy dispersive spectra (XEDS) were acquired at 15 kV on a JEOL 5800 LV Scanning Electron Microscope equipped with a ultra-thin window (UTW) X-ray detector.

Received: May 23, 2007
Revised: August 1, 2007
Published online: September 20, 2007

Keywords: bimetallic clusters · electron microscopy · heterogeneous catalysis · hydrogenation · nanoparticles

[1] S. Hermans, R. Raja, J. M. Thomas, B. F. G. Johnson, G. Sankar, D. Gleeson, *Angew. Chem.* **2001**, *113*, 1251; *Angew. Chem. Int. Ed.* **2001**, *40*, 1211.
[2] J. M. Thomas, B. F. G. Johnson, R. Raja, G. Sankar, P. A. Midgley, *Acc. Chem. Res.* **2003**, *36*, 20.
[3] S. Hermans, B. F. G. Johnson, *Chem. Commun.* **2000**, 1955.
[4] a) B. A. Riguetto, C. E. C. Rodrigues, M. A. Morales, E. Baggio-Saitovitch, L. Gengembre, E. Payen, C. M. P. Marques, J. M. C. Bueno, *Appl. Catal. A* **2007**, *318*, 70; b) G. W. Huber, J. W. Shabaker, J. A. Dumesic, *Science* **2003**, *300*, 2075; c) M. Guidotti, V. Dal Anto, A. Gallo, E. Gianotti, G. Peli, R. Psaro, I. Sordelli, *Catal. Lett.* **2006**, *112*, 89; d) M. S. Holt, W. L. Wilson, J. H. Nelson, *Chem. Rev.* **1989**, *89*, 11; e) J. N. Coupé, E. Jordão, M. A. Fraga, M. J. Mendes, *Appl. Catal. A* **2000**, *199*, 45; f) S. M. Santos, A. M. Silva, E. Jordao, M. A. Fraga, *Catal. Commun.* **2004**, *5*, 377; g) M. Toba, S. Tanaka, S. Niwa, F. Mizukami, Z. Koppany, L. Guczi, K.-Y. Cheah, T.-S. Tang, *Appl. Catal. A* **1999**, *189*, 243.
[5] a) B. Coq, F. Figueras, C. Moreau, P. Moreau, M. Warawdekar, *Catal. Lett.* **1993**, *22*, 189; b) R. A. van Santen, M. Neurock, *Molecular Heterogeneous Catalysis: A Conceptual and Computational Approach*, Wiley-VCH, New York, **2006**.
[6] R. D. Adams, B. Captain, W. Fu, M. D. Smith, *Inorg. Chem.* **2002**, *41*, 5593 – 5601.
[7] A. B. Hungria, R. Raja, R. D. Adams, B. Captain, J. M. Thomas, P. A. Midgley, V. Golvenko, B. F. G. Johnson, *Angew. Chem.* **2006**, *118*, 4900 – 4903; *Angew. Chem. Int. Ed.* **2006**, *45*, 4782 – 4785.
[8] P. D. Nellist, S. J. Pennycook, *Adv. Electron. Electron Phys.* **2000**, *113*, 147 – 203.
[9] a) G. W. Crabtree, M. S. Dresselhaus, M. V. Buchanan, *Phys. Today* **2004**, *57*, 39 – 44; b) J. M. Ogden, *Phys. Today* **2002**, *55*, 69 – 75; c) J. Ogden, *Sci. Am.* **2006**, *295*, 94 – 101; d) S. Satyapal, J. Petrovic, G. Thomas, *Sci. Am.* **2007**, *296*, 81 – 87; e) P. P. Edwards, V. L. Kuznetsov, W. I. F. David, *Philos. Trans. R. Soc. London* **2007**, *365*, 1043.

